Some European Developments in Welding Consumables

L. Karlsson† and H. K. D. H. Bhadeshia*

November 1, 2010

†ESAB AB, Göteborg, Sweden
*University of Cambridge, U. K.

Abstract

This paper represents a selected survey of incisive research on novel welding consumables which contribute to the structural integrity of advanced engineering structures. It is evident that there are tremendous advances to be made by applying the most sophisticated instrumentation available to Materials Science, together with theory and insight based on metallurgical experience. We congratulate the Japan Welding Society for organising this special issue of their journal.

1 High Strength Steel Weld Metals

The increasing use of steels with a strength in excess of 700 MPa has led to a demand for stronger welding consumables. In contrast to production of wrought steel, the strength and toughness of weld metals must generally be achieved by means of alloying. Whereas there are many ways of increasing the strength, doing so while maintaining good toughness has proven to be more challenging. And the properties achieved must also be robust in the sense that they should not be sensitive to practical variations in the welding parameters. Other risks become more prominent at high strengths, for example, fatigue resistance and hydrogen embrittlement.

The traditional argument is that the concentration of solutes added to ferritic weld metals must be kept to a minimum in order to avoid martensite and avoid the risk of brittle fracture. Weld metal yield strengths therefore usually lie in the range 350–550 MPa, with occasional higher values achieved at the expense of toughness. The microstructure of such weld metals consists of mixtures of allotriomorphic ferrite (α), Widmanstätten ferrite (α_w), acicular ferrite (α_a) and the so–called microphases (small quantities of retained austenite and martensite) [1, 2]. Allotriomorphic ferrite is weak, and Widmanstätten ferrite suffers from poor toughness. This leaves acicular ferrite as a good strengthener with its ability to deflect cracks. However, welds containing mostly acicular ferrite still do not meet the requirements of the strongest of structural steels, as illustrated in Fig. 1 [3].

We present in this review a variety of European efforts to make reliable welding alloys which are practicable in commercial practice.

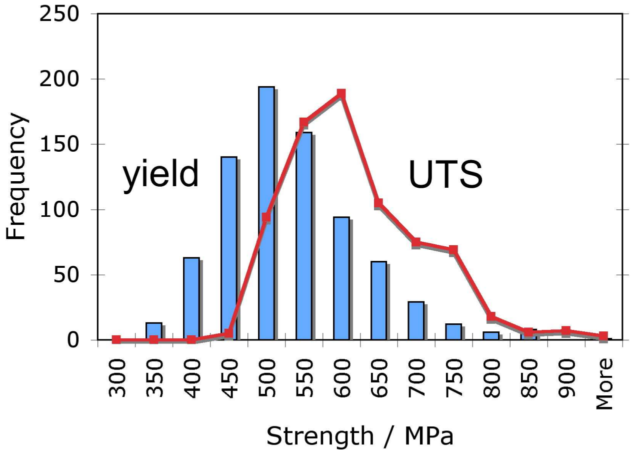

Figure 1: Distribution of strength in ferritic steel weld metals, incorporating data from some 800 welding alloys. UTS stands for the ultimate tensile strength. Data from [4].

1.1 Oxygen Content

To achieve strength in excess of 700 MPa in yield it is necessary to work with microstructures are largely bainitic or martensitic, meaning that acicular ferrite can no longer be relied on to achieve the correct combination of mechanical properties. Acicular ferrite relies on the presence of oxides as nucleation sites; phases such as martensite do not, in which case the oxides have the potential of initiating fracture and the oxygen content must be minimised. This is apparent in Fig. 2 [5–10]. Optimising high strength weld metals therefore requires precise control and understanding of minor alloying elements and impurities, minimisation of oxygen content and thereby the amount and size of inclusions.

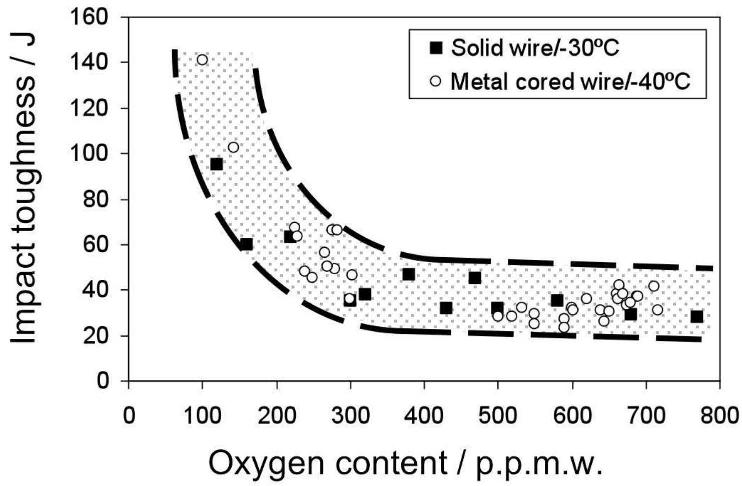

Figure 2: Effect of oxygen content on Charpy–V impact toughness of supermartensitic weld metals on. Weld metals produced with different welding processes and different consumables all fall within the same scatter band [6].

1.2 Microstructural Constituents

In addition to the classical microstructural constituents such as bainite, martensite and the softer ferrite variants associated with leaner compositions a microstructural constituent previously reported in high strength steels Coalesced Bainite has recently also been identified in weld metals (Figure 3) [11–14]. It forms by the coalescence of finer bainite platelets, each of which is separately nucleated but in the same crystallographic orientation during prolonged growth. EBSD studies and FIB sectioning techniques have proved that coalesced bainite grains can be several micrometers in all directions [15]. There is evidence that this constituent forms at large driving forces [16], that is at relatively low temperatures. It has also been observed that it is more likely to occur when the bainite and martensite start temperatures are close. As this coarse phase is detrimental to mechanical properties, care has to be taken when designing new high strength welding alloys to ensure it does not form in significant amounts.

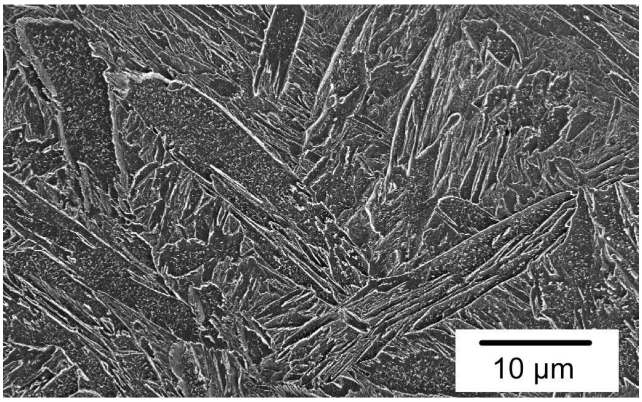

Figure 3: Large coalesced bainite grains in the last bead of a 0.08C–10Cr–1Ni–0.3Mo wt% high strength weld metal with 910 MPa in yield strength.

Having established which microstructural constituents form for a given weld metal composition the next step is to correlate these to properties and how welding procedures affect the relative amounts.

1.3 Robustness

Although well balanced mixed martensitic/bainitic/ferritic microstructures can offer high strength and good toughness, the microstructure and hence the properties, tend to be sensitive to the cooling rate [17–20] as exemplified in Fig. 4 for weld metals with different Ni–contents.

Different approaches can be adopted to counteract or minimise this effect. One approach is to define an operational window within which high strength and good toughness can be achieved. A second approach is to achieve a greater tolerance to variations in the weld thermal cycle with a higher alloy content and perhaps a radical departure from established alloying practices as discussed later in the text.

The first approach is exemplified for weld metals deposited with a high strength MMA electrode (ESAB OK 75.78), with nominal composition Fe-0.05C-0.3Si-2Mn-3Ni-0.5Cr-0.6Mo wt% (Fig. 4) [14]. Effects of welding parameters on properties and microstructures were characterised (Fig. 5) for a range of cooling rates using high resolution scanning electron microscopy and the transformation behaviour was assessed from cooling curves.

As the next step a continuous cooling diagram was constructed from cooling curves. The transformation temperatures were displayed as a function of cooling time between 800 and 500°C, as this is often used to characterise weld thermal cycles (Fig. 6).

Mechanical properties correlated with observed microstructure and transformation behaviour. Results suggest high strength and good toughness for cooling rates between 800 and 500°C of about 3 s to 13 s. A fine microstructure will then form with varying proportions of martensite, lower bainite, coalesced bainite and fine upper bainite. The recommended cooling rate window will not impose a limitation in practise, as welding procedures resulting in extreme cooling rates are rarely desirable. A more practical concern is that transformation behaviour and properties in real weldments always are affected by dilution, as modern high strength steels are rather lean in composition. Ways of dealing with this and maintain properties for varying dilution levels are therefore of interest.

1.4 Alternative Alloying Approaches

A neural network model was created with the task of exploring new compositions which might be suitable for high strength steel weld metals as described in [21, 22]. Based on predictions and preliminary tests, a nominal weld metal composition of 0.06C, 7Ni, 0.5Mn wt% was found to offer stable and attractive properties at a high level [11, 23, 24]. The more highly alloyed 7Ni weld metal represents a different approach producing a microstructure consisting mainly of bainite with a limited effect of cooling time on martensite content. Variations in properties are listed in Fig. 4 and are listed in Table 1. Figure 7 shows that the impact strength is high and varies little with cooling rate.

Table 1: Chemical composition (wt%) and mechanical properties of the nominally 7Ni high–strength welding alloy.

C	Si	Mn	Cr	Ni	Mo	O	N
0.051	0.38	0.54	0.15	6.70	0.40	0.330	0.130

Ultimate strength / MPa	0.2% proof / MPa	Elongation / %	Charpy (-40°C) / J	$\Delta t_{8/5}$ / s
888	850	20.4	96	11

1.5 Role of Inclusions

Not only has the weld metal composition to be carefully designed to minimise formation of undesirable microstructural constituents. Inclusions also play an important role for formation of acicular ferrite as well as affects bainite formation in more highly alloyed high strength weld metals. Minor variations of alloying elements or deoxidising elements can therefore have a profound effect on the

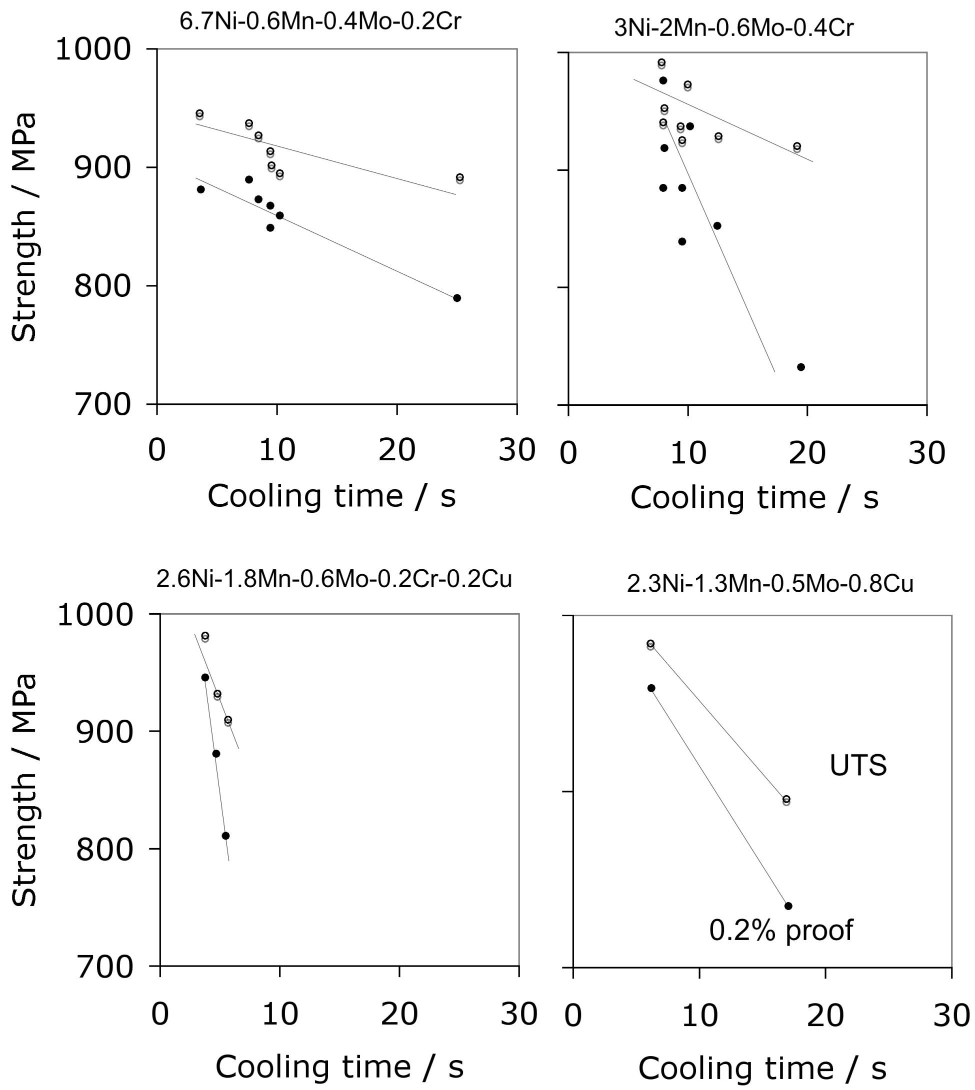

Figure 4: Strength as a function of cooling time between 800 and 500°C for weld metals with Ni contents in the range 2.3–6.7 wt%, [18].

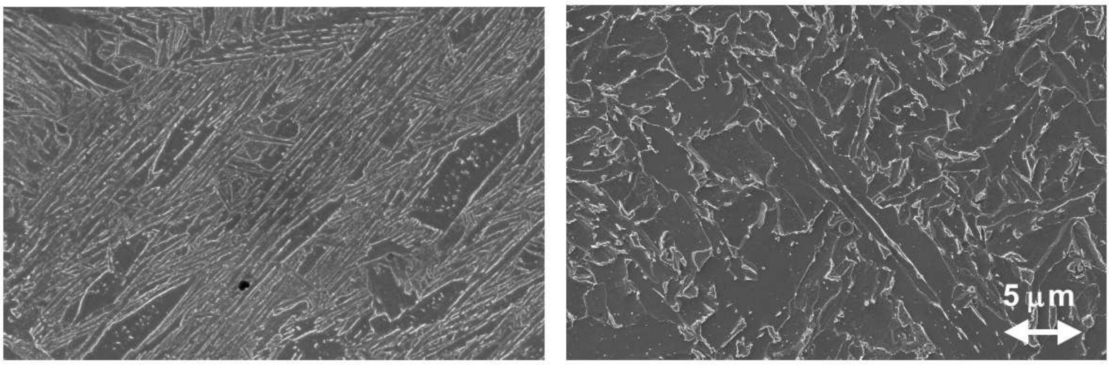

Figure 5: FEGSEM micrographs presenting an overview of the as-deposited last bead microstructure for two different cooling times. Lower bainite, martensite and coalesced bainite are the main constituents in the rapidly cooled weld metal on the left, whereas the more slowly cooled structure consists largely of upper bainite.

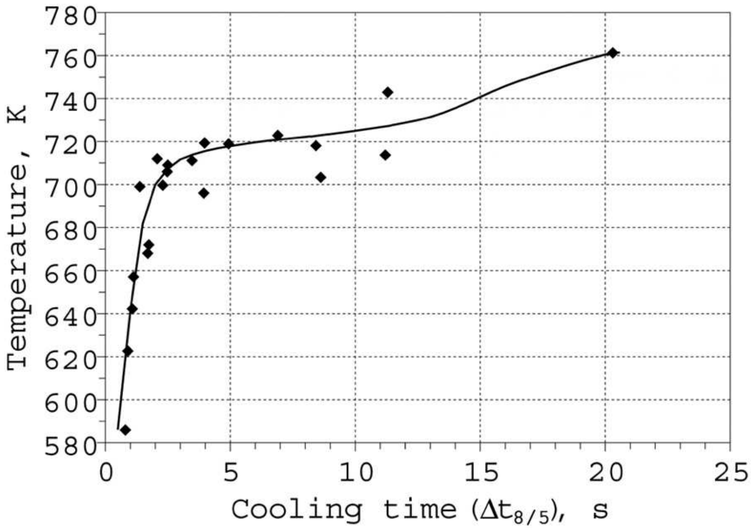

Figure 6: Experimental CCT–diagram for OK 75.78 displaying transformation start temperatures as a function of cooling time between 800C and 500C. Transformation temperatures gradually increase with cooling time above 3 s and decrease rapidly for shorter cooling times.

microstructure and hence properties. In particular for flux shielded processes such manual metal arc (MMA), flux cored arc welding (FCW) and submerged arc welding (SAW) this poses challenges in combination with striving for lower oxygen levels.

Non–metallic inclusions in weld metals often consist of several different phases with varying composition and structure [2]. Figure 8 shows an example of the morphology of a typical complex inclusion in a high strength weld metal. Several mechanisms have been suggested for the role of inclusions in nucleation of ferrite [1, 7]; the presence of Mn depletion zones [25], induced strain due to difference in thermal expansion [26] and lattice mismatch [27], among others. It is however not yet fully clear whether one or several of these mechanism or other effects such as formation of Ti-layers as discussed below are of greatest importance in high strength largely bainitic or martensitic microstructures.

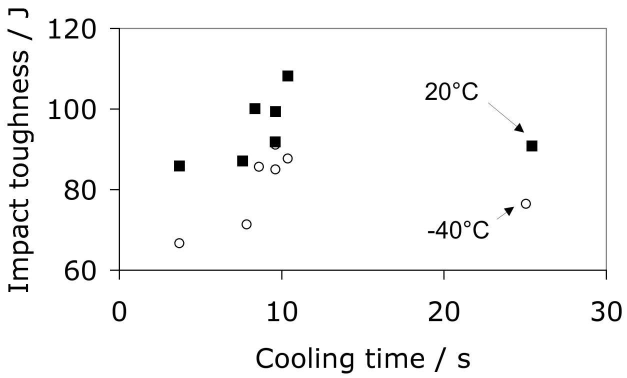

Figure 7: Impact toughness as a function of cooling time ($\Delta t_{8/5}$) for a highly alloyed high strength weld metal.

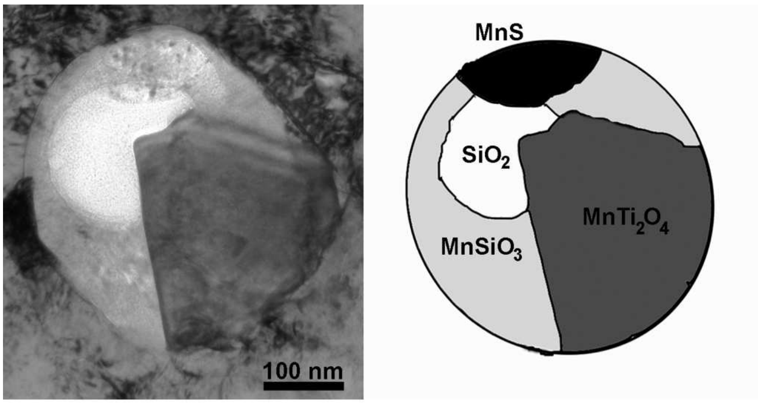

Figure 8: a) Bright field transmission electron micrograph of an inclusion. b) Schematic representation of the inclusion, showing the morphology of present phases.

For many of the suggested theories, a resulting orientation relationship between a specific phase and an adjacent ferrite grain should be expected. A dark-field transmission electron micrograph of a $MnTi_2O_4$–spinel phase in an inclusion and an adjacent ferrite grain is shown in Figure 9a. The corresponding diffraction pattern is shown in Figure 9b, giving the orientation-relationship between the spinel structure and the adjacent ferrite grain to be: $[112]_\alpha||[112]_{\text{spinel}}$ and $[11\bar{1}]ferrite||[\bar{3}11]_{\text{spinel}}$. This could then suggest that in this case, the $MnTi_2O_4$–spinel phase have been responsible for the nucleation of the ferrite grain on the inclusion.

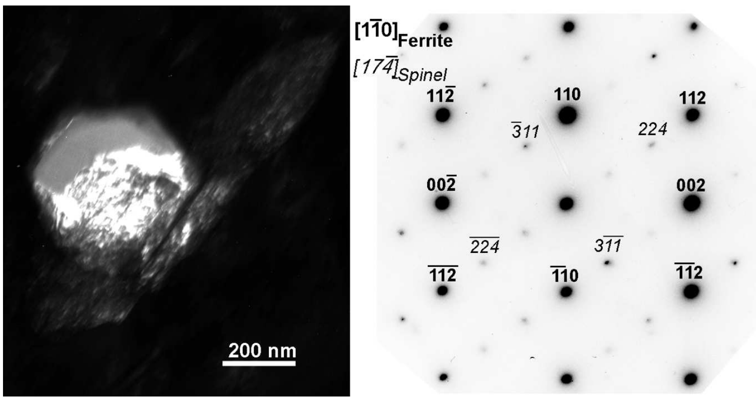

Figure 9: a) Dark field transmission electron micrograph of an inclusion and an adjacent ferrite grain. b) The corresponding selected area electron diffraction pattern with indexed reflection for both the ferrite grain and the MnTi2O4-spinel phase of the inclusion. Extra reflections are due to double diffraction.

Another recently reported finding is the presence of a Ti containing, possibly TiO, film in the matrix-inclusion interface, which enhances the nucleation at inclusions for a certain composition

[28]. Figure 10 shows a micrograph of an inclusion along with the distribution of titanium and oxygen. A thin titanium–rich layer is clearly seen at the inclusion-matrix boundary. The presence of oxygen in the same layer could, however, not be determined conclusively.

Further knowledge is definitely needed in order to determine the exact role of complex inclusions, with their different phases, and segregated layers at interfaces in the nucleation on inclusions.

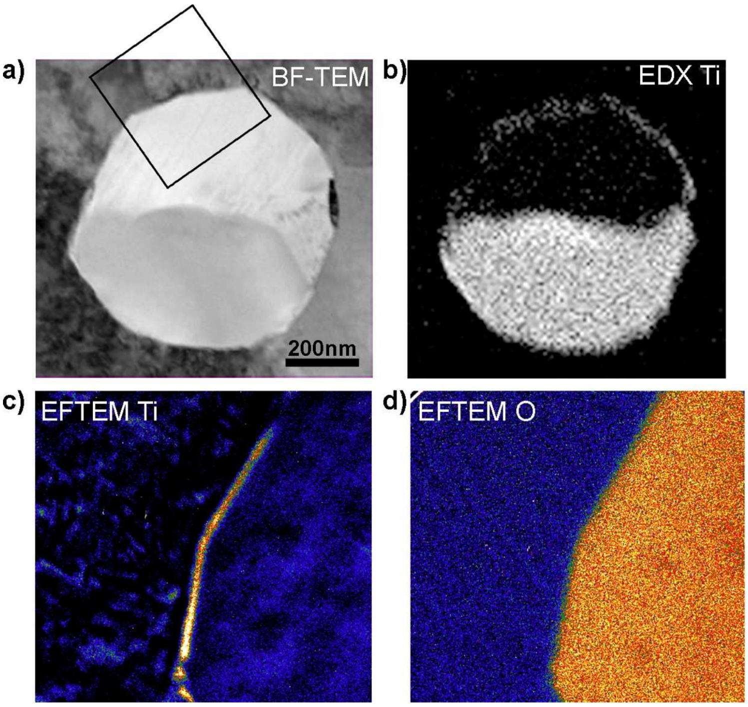

Figure 10: Bright field transmission electron micrograph of an inclusion. An EDX titanium map of the inclusion is shown in b). Energy filtered transmission electron micrographs of titanium and oxygen elemental maps are shown in c) and d), respectively. The maps were recorded over the area marked with a black square in a).

1.6 Microstructural Characterisation

Significant developments have been made in understanding the effect of microstructure on mechanical properties of high strength weld metals [11, 23, 24, 29–31]. Through the use of high resolution field emission gun scanning electron microscopy (FEGSEM) in combination with light optical microscopy (LOM) and transmission electron microscopy (TEM) the individual microstructural constituents can be identified (6). Figure 11 shows an example of a 7Ni weld metal (composition as presented earlier) where SEM with EBSD has been used to reveal the true grain structure in order to enable a better interpretation in the optical microscope.

A comprehensive understanding of the material is key in achieving desired properties and enabling a continuing advance towards higher strength levels. It is often the case that substantial progress is made when a previously unseen correlation is found in empirical data, either by accident or deliberate hypothesis testing. Sometimes such correlations are hidden in the non-linearity of the data and revealed through the use of new statistical tools. Other times the pattern is not revealed until the experimental techniques have developed the resolution and accuracy needed to expand the measurement range. The development of EBSD has resulted in a technique capable of rapidly

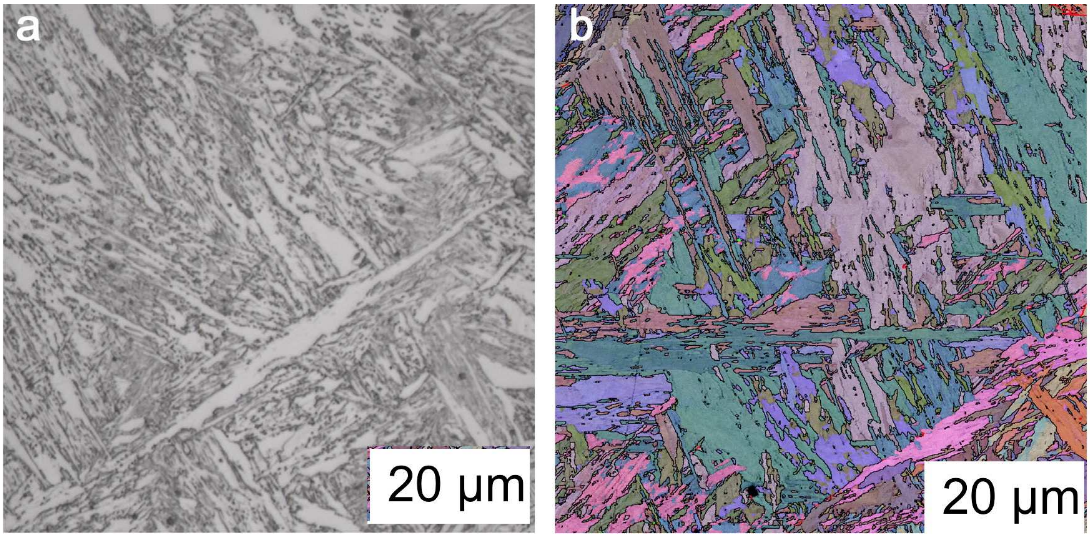

Figure 11: (a) LOM micrograph showing the etched microstructure of a 7Ni weld metal. (b) EBSD orientation map from the same microstructure.

performing vast amounts of orientation measurements, thereby allowing for increased accuracy when determining average quantities like the mean orientation of crystallographic variants.

It is well established that the orientation relationship (OR) between austenite and the various ferrite constituents is irrational but generally in the vicinity of the Kurdjomov–Sachs (KS) or Nishiyama–Wasserman (NW) ORs [32]. For example, in low carbon martensite the OR is close to KS whereas in high carbon martensite it is closer to NW [33]. By characterising a microstructure in terms of an accurate mean OR and studying the distribution of orientations around this mean it should be possible to discern more subtle details concerning the displacive transformation products. This kind of characterisation requires a large number of orientation measurements to be performed on a very local scale, a task for which the EBSD technique is well suited. To determine the OR of a particular alloy a mathematical model of the lattice transformation can be fitted to the collected orientation data and the results can be visualised as pole figures or as parameters of some rotation representation (Fig. 12) [34, 35].

Figure 13 shows an example where calculated poles of one Bain zone are superimposed on the experimental Bain zone obtained by EBSD measurement in a single prior austenite grain of a 7Ni weld metal. An accurately determined mean OR can then also be used to facilitate further evaluation of orientation data, *e.g.* when reconstructing the prior austenite grain structure.

As the development towards higher strength levels progresses, an increasing number of parameters are becoming involved in the design of welding consumables. It is therefore inevitable that brute force approaches to development, in the future will become increasingly resource consuming and the need for phenomenological understanding combined with modelling even greater than before.

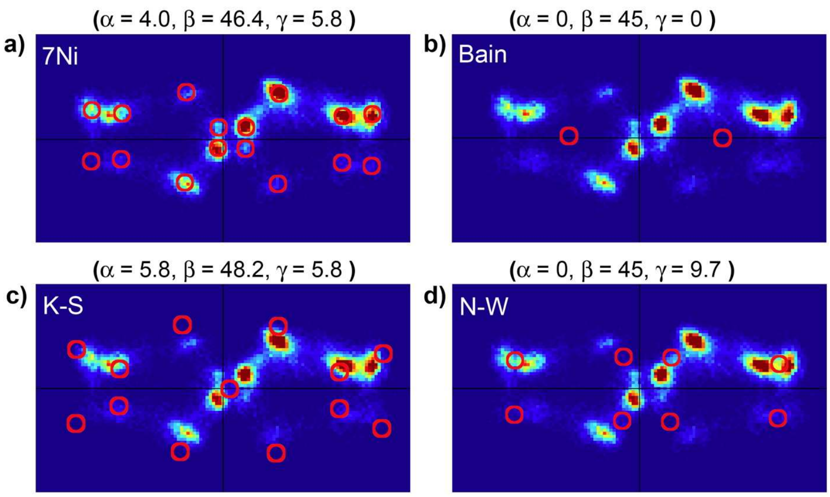

Figure 12: Bain zone from a {111} experimental pole figure, colour-coded with respect to intensity. Theoretical poles for the different ORs 7Ni (best fit), Bain, K-S and N-W are marked with red circles in a)-d), respectively. The Euler angles are also given for each OR.

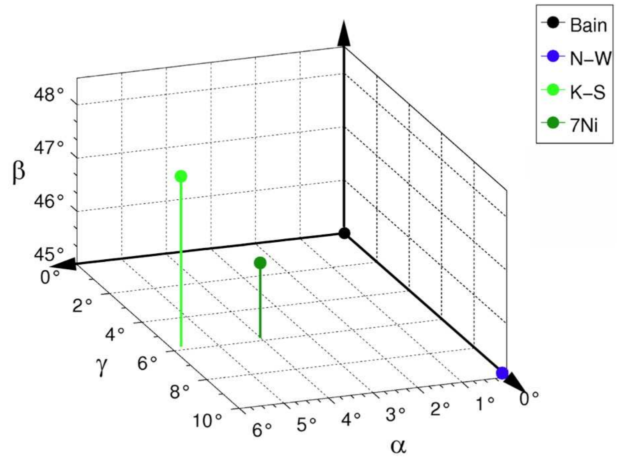

Figure 13: . Euler space representation of the OR between austenite and ferrite in a 7Ni weld metal. Common rational ORs are also displayed for the purpose of reference.

2 Stainless Steels

With greater attention on achieving low long–term maintenance costs, increasing environmental awareness and greater concern with life cycle costs, the market for stainless steel continues to improve [36]. Two trends in stainless steel development can be recognised. On the one hand the recent rapid fluctuations in Ni and also Moprices have lead to the introduction and increased use of leaner less expensive grades. In particular so-called lean duplex stainless steels have attracted a lot of interest as cost efficient alternatives to standard austenitic grades such as 304L and 316L. Some of the Ni in these steels is often replaced by a combination of Mn and N in order to keep the alloying cost at a minimum whilst maintaining strength, corrosion resistance and a suitable phase balance (Table 2).

Table 2: Chemical compositions (wt%) of some stainless steels. $PRE_N = Cr + 3.3Mo + 16N$.

Steel type	AISI/UNS	EN	Cr	Mo	Ni	Mn	Cu	N	PRE_N
Austenitic	304L	1.4307	18		9	1			18
	316L	1.4401	17	2	11	1			24
	904LN	1.4339	20	4	25	1	1.5	0.1	35
"Lean" duplex	S 32001	1.4482	20		1.6	5	0.3	0.13	22
	S 32101	1.4162	21.5	0.3	1.5	5		0.22	26
	S 32304	1.4362	22.5	0	4.8	1		0.1	25
	S 32003		21.5	1.8	3.5	2		0.18	30
22%Cr duplex	S 32205	1.4462	22	3	6	1		0.17	35

On the other hand there is also continuos development of new specialised highly alloyed grades intended for very corrosive environments and high temperatures. A trend in both austenitic and duplex stainless steel production (the "super-trend" and recently also "hyper-trend") has for more than two decades been the introduction of grades with higher alloy contents to meet the demand for higher corrosion resistance in special applications. Commonly Cr and Mo contents are increased to improve corrosion resistance although lately N and to some extent W have become important alloying elements.

2.1 Welding Consumable Development

For obvious reasons consumable manufacturers must follow the lead of steel makers in formulating new alloys. However, as a welding operation can have significant effects on mechanical properties and corrosion performance steel will not become widely accepted and used unless they can be successfully welded without too many limitations. One example is given for development of consumables for lean duplex stainless steels and one for very highly alloyed Ni-base alloys.

2.1.1 Lean duplex consumables

Welding consumables for duplex stainless steels need to be higher in elements promoting austenite formation, compared to the corresponding steel grade, to avoid excessively high weld metal ferrite contents. At the same time it is important to ensure appropriate mechanical properties and corrosion resistance. Weld metal design therefore requires a careful balancing of alloying elements.

Microstructures and properties of lean duplex weld metals produced with experimental covered electrodes or metal-cored wires were evaluated in a recent study aiming at optimising the composition [37, 38]. Various compositions with 21.5-24 wt%Cr with different levels of Ni and Mn in combination with N were selected to produce a minimum PRE_N value of 26. The electron backscattered diffraction (EBSD) technique combined with scanning electron microscopy (SEM) was used to explore relations between weld metal morphology and crystallographic orientation relationships between ferrite and austenite.

Depending on composition lean duplex weld metals solidify either fully as ferrite producing a "typical Widmanstätten-type" microstructure or in a mixed mode with ferrite as the leading phase and austenite forming interdendritically (see example in Fig. 14).

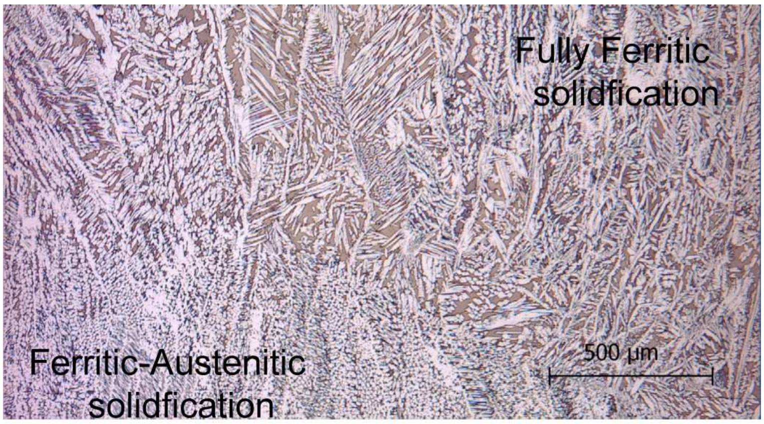

Figure 14: Lean duplex weld metal with regions of Widmanstätten-type austenite typical of a fully ferritic solidification (top) and regions having a morphology with ferrite located mainly interdendritically and forming an almost continuos network typical of mixed austenitic-ferritic solidification (bottom).

Impact toughness varied markedly between the weld metals. Several factors, many of those interacting, are known to affect impact toughness. This makes it difficult to visualise effects in simple diagrams looking at one factor only. However, plotting ferrite content against impact toughness (Fig. 15) and separate weld metals according the solidification mode clearly illustrates that this and the resulting ferrite morphology has to be considered. Weld metals solidifying completely as ferrite showed less scatter and generally had toughness on a higher level. The question should then be asked how solidification mode, morphology and texture could affect impact toughness. As ferrite is the less ductile of the two phases it is reasonable to primarily focus on aspects of ferrite morphology and texture.

The ferrite morphology seems more important than the ferrite/austenite relative orientation. A contributory factor in a mixed mode solidification structure is most likely relation between ferrite morphology and orientation of preferred cleavage planes {100}. As the preferred growth direction in solidification is [100] the planes of easiest cleavage, which are {100}, tend to be aligned with the ferrite. This alignment effect is probably of less importance in the ductile regime but can be critical for the resulting toughness below the ferrite ductile to brittle transition temperature.

The influence of the relative orientation between ferrite and austenite is less clear but it was attempted to see if there were differences between weld metals with the two types of solidification in the tendency to form randomly oriented phase boundaries or specific orientation relationships such as Nishiyama–Wasserman (NW) or Kurjdumov–Sachs (KS). It was decided to examine whether the grain boundaries were close to any of these orientation relationships rather than looking for exact matches as these tend to be irrational in real life [32]. Any match within 4° deviation from

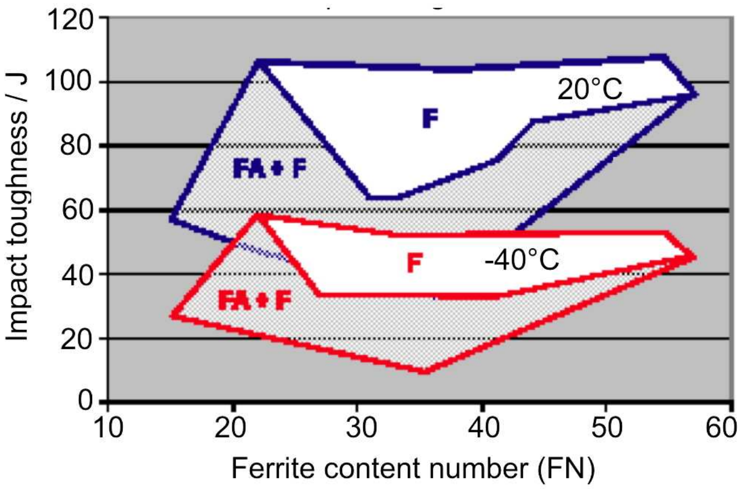

Figure 15: Impact toughness scatter bands for lean duplex weld metals with a fully ferritic solidification (F) and those with regions having a morphology with ferrite located mainly interdendritically and forming an almost continuous network typical of mixed austenitic-ferritic solidification (FA). The minimum values and scatter increase significantly with mixed mode solidification.

the perfect relationships was therefore classified as either NW or KS and all others as random grain boundaries. As summarised in Fig. 16 EBSD it was found that most of the austenite was near either the KS or the NW relationships with adjacent ferrite in line with observations in other studies [39]. More of the phase boundaries in the mixed mode solidification regions had a random orientation relationship compared to after fully ferritic solidification. It was also seen that boundaries more frequently were close to the NW relationship after fully ferritic solidification whereas KS was more common after a mixed mode solidification.

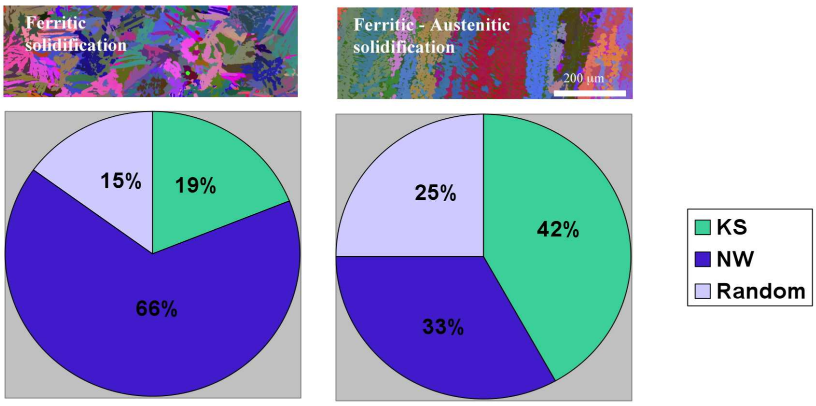

Figure 16: EBSD orientation maps (top) and classification of austenite/ferrite boundary orientations (below) for weld metals with a fully ferritic solidification (left) and mixed ferritic-austenitic solidification (right). More phase boundaries had a random orientation relationship after mixed mode solidification. The NW relationship was most frequent after fully ferritic solidification whereas KS was more common after a mixed mode solidification

Although not discussed in detail here it was concluded that in addition to a fully ferritic solidification also a sufficient Ni-content is necessary to produce acceptable and reproducible impact toughness at room and sub-zero temperatures. A composition of 23-24Cr, 7-8Ni and 0.12-0.16N wt% was found well suited to fulfil all requirements.

Development of duplex grades is ongoing and weldability is an issue much studied [41] and discussed. Current issues are for example the effects of W-alloying [40] and the application of low-energy input welding methods on properties [41].

2.2 Highly Alloyed Ni–base Consumables

The adverse effect of segregation during solidification of stainless steel weld metals on corrosion resistance is well known and over-alloying is a well-established practise to counteract this phenomenon [42]. However, as alloying content increases precipitation of deleterious phases becomes unavoidable and more structurally stable nickel-based consumables are employed. Currently the corrosion resistance of the most highly alloyed austenitic grades is difficult to match even with nickel-based consumables. An interesting development is the use of modern modelling tools such as ThermoCalc [43] in alloy development to find new routes around what might seem to be fundamental problems (Fig. 17).

Thermodynamic calculations were performed to find potential alloys of interest. Experimental weld metals were then produced, microstructures were characterised and local alloy content variations were quantified. These experiments verified that a higher total alloying content can be tolerated in nickel-based weld metal if a combination of W and Mo is used rather than either of the two elements alone [44]. An example is illustrated in Fig. 18 showing that whereas Mo is enriched in interdendritic regions a corresponding W-depletion occurs resulting in an overall more even distribution of alloying elements, better resistance to localised corrosion and less risk of precipitation.

3 Cancellation of Residual Stresses

Residual stresses are an anathema in welds because they are associated with distortion [45], they limit the magnitudes of the external stress that a weld can support and influence the life of the joint in a variety of scenarios [46–48].

There are a number of groups developing welding consumables capable of mitigating the residual stresses that develop when the liquid metal filling a joint solidifies and contracts [49–63]. The mechanism of stress cancellation relies on the solid–state transformation of the weld metal into bainite or martensite at a sufficiently low temperature, such that the transformation plasticity cancels any strain due to thermal contraction. It is believed that the extent of this relief is dependent on the selection of particular crystallographic variants of the transformation product which are thermodynamically favoured in the particular environment of the accumulating residual stress [64].

Much of the work has focused on welding materials for ferritic steels containing relatively low concentrations of solutes. In contrast, the purpose of the work presented here was to develop a corresponding alloy for welding austenitic stainless steels. The weld metal must therefore contain a critical concentration of chromium in order to ensure a 'stainless' character through the spontaneous formation of a protective chromia film provided a trace of oxygen or oxidising agent is present. It must at the same time be able to transform into martensite at a relatively low temperature, so that

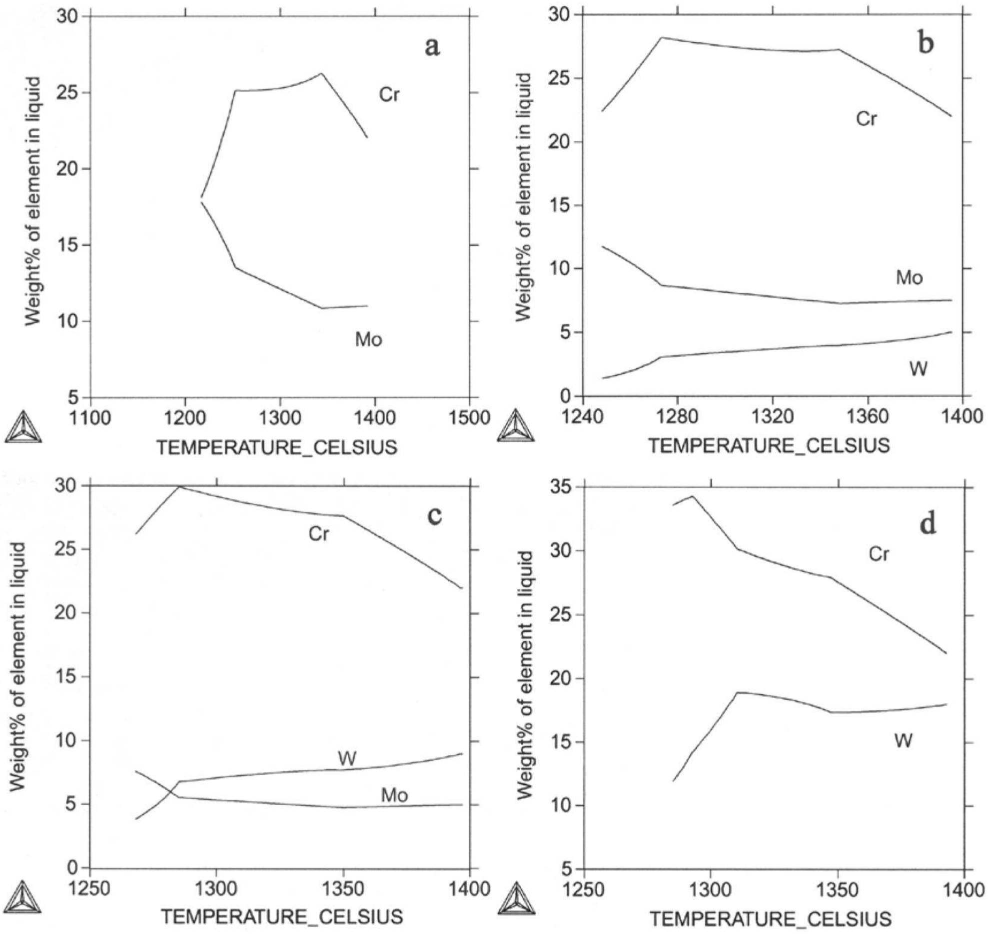

Figure 17: Thermo-Calc results from the Scheil calculations showing the concentration of elements in the liquid during solidification. At lower temperatures changes occur because of precipitation, which is probably too slow to take place in practise. The base composition was Ni - 0.05C, 0.5Si, 1Mn and 22Cr wt%, with varying amounts of Mo and W. a) 11Mo, b) 7.5Mo-5W, c) 5Mo-9W and d) 18W.

the resulting plasticity can be exploited to compensate for any accumulated stress. Such a *stainless steel* welding consumable has been developed, which solidifies as δ–ferrite, transforms almost entirely into austenite which then undergoes martensitic transformation at a low temperature of about 260°C. At the same time, the carbon concentration has been kept to a minimum to avoid phenomena such as sensitisation. The measured mechanical properties, especially toughness, seem to be significantly better than commercially available martensitic stainless steel welding consumables, and it has been demonstrated that the use of the new alloy reduces distortion in the final joint [65].

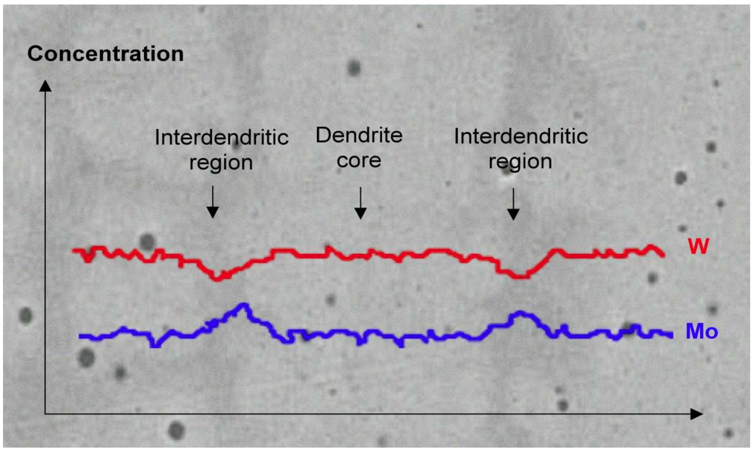

Figure 18: Concentration profiles for W and Mo across dendrites in a Ni-based weld metal. Mo is enriched in interdendritic regions whereas W is depleted resulting in a more even distribution of alloying elements and thereby better corrosion resistance. Dendrite spacing is approximately 10 μm.

4 Conclusions

It is evident from this narrow survey that there are exciting developments in the design of alloys which act as filler metals during welding. The thrill comes not only from the achievement of individual mechanical or chemical properties, but of unusual combinations of properties. The intensity of research, which exploits all of the modern techniques of science ranging from Charpy tests to synchrotron analysis, and techniques capable of looking at individual atoms, is a reflection of the fact that the goals are difficult. We hope that this paper gives a flavour of the progress being made, particularly in research within the European domain.

Acknowledgments

The assistance of J. Börjesson and J. Zachrisson, (ESAB AB, Sweden) in preparing the manuscript is gratefully acknowledged.

References

[1] D. J. Abson and R. J. Pargeter. Factors influencing the as–deposited strength, microstructure and toughness of manual metal arc welds suitable for C–Mn steel fabrications. *International Materials Reviews*, 31:141–194, 1986.

[2] S. S. Babu, J. W. Elmer, S. A. David, and M. Quintana. In situ observations of nonequilibrium austenite formation during weld solidification of a FeCAlMn low alloy steel. *Proceedings of the Royal Society A*, 458:811–821, 2002.

[3] H. K. D. H. Bhadeshia. Strong ferritic-steel welds. *Materials Science Forum*, 539–543:6–11, 2007.

[4] T. Cool, H. K. D. H. Bhadeshia, and D. J. C. MacKay. The yield and ultimate tensile strength of steel weld metals. *Materials Science and Engineering A*, 223A:186–200, 1997.

[5] L. Karlsson, W. Bruins, C. Gillenius, S. Rigdal, and M. Goldschmitz. Matching composition supermartenstic stainless steel welding consumables. In *Supermartensitic Stainless Steels '99*, pages 172–179, Brussels, Belgium, 1999.

[6] L. Karlsson, S. Rigdal, and P. Dyberg. Submerged arc welding of supermartensitic stainless steels: Good as welded toughness – realistic or not? In *Supermartensitic Stainless Steels '99*, pages 44–53, Brussels, Belgium, 2002.

[7] T. Koseki and G. Thewlis. Inclusions in welds. *Materials Science and Technology*, 21:867–879, 2005.

[8] M. Goldschmitz, L. Karlsson, R. Pedersen, S. Rigdal, and J. van den Broek. Developments in the welding of supermartensitic stainless steels: recent developments and applications. *Welding International*, 18:543–549, 2004.

[9] S. Terashima and H. K. D. H. Bhadeshia. Changes in toughness at low oxygen concentrations in steel weld metals. *Science and Technology of Welding and Joining*, 11:509–516, 2006.

[10] S. Terashima and H. K. D. H. Bhadeshia. Size distribution of oxides and toughness of steel weld metals. *Science and Technology of Welding and Joining*, 11:580–582, 2006.

[11] E. Keehan, L. Karlsson, and H.-O. Andrén. Influence of C, Mn and Ni on strong steel weld metals: Part 1, effect of nickel. *Science and Technology of Welding and Joining*, 11:1–8, 2006.

[12] E. Keehan, L. Karlsson, H. K. D. H. Bhadeshia, and M. Thuvander. Electron backscattering diffraction study of coalesced bainite in high strength steel weld metals. *Materials Science and Technology*, 24:1183–1188, 2008.

[13] J. H. Pak, H. K. D. H. Bhadeshia, L. Karlsson, and E. Keehan. Coalesced bainite by isothermal transformation of reheated weld metal. *Science and Technology of Welding and Joining*, 13:593–597, 2008.

[14] E. Keehan, J. Zachrisson, and L. Karlsson. Influence of cooling rate on microstructure and properties of high strength steel weld metal. *Science and Technology of Welding and Joining*, 15:233–238, 2010.

[15] E. Keehan, L. Karlsson, H. K. D. H. Bhadeshia, and M. Thuvander. Three–dimensional analysis of coalesced bainite using focused ion beam tomography. *Materials Characterization*, 59:877–882, 2008.

[16] H. K. D. H. Bhadeshia, E. Keehan, L. Karlsson, and H. O. Andrén. Coalesced bainite. *Transactions of the Indian Institute of Metals*, 59:689–694, 2006.

[17] D. J. Widgery, L. Karlsson, M. Murugananth, and E. Keehan. Approaches to the development of high strength steel weld metals. In *2nd International symposium on high strength steel, Norway*, pages 1–10, Brussels, Belgium, 2002. The European Coal and Steel Community.

[18] L. Karlsson, E. Keehan, H.-O. Andrén, and H. K. D. H. Bhadeshia. Development of high strength steel weld metals – potential of novel high-ni compositions. In *Proceedings of Eurojoin 5*, page paper V6, Vienna, Austria, 2004. EWA and SZA.

[19] W. Wang and S. Liu. Alloying and microstructural management in developing SMAW electrodes for HSLA-100 steel. *Welding Journal, Research Supplement*, 81:132s–145s, 2002.

[20] D. P. Fairchild, M. L. Macia, N. V. Bangaru, and J. Y. Koo. Girth welding development for x120 linepipe. In *Proceedings of the 13th International Offshore and Polar Engineering Conference*, pages 26–35, Philidelphia, USA, 2003. ASME.

[21] M. Murugananth, H. K. D. H. Bhadeshia, E. Keehan, H. O. Andrén, and L. Karlsson. Strong and tough steel welds. In H. Cerjak and H. K. D. H. Bhadeshia, editors, *Mathematical Modelling of Weld Phenomena 6*, pages 205–230, 2002.

[22] E. Keehan, H.-O. Andrén, L. Karlsson, M. Murugananth, and H. K. D. H. Bhadeshia. Microstructural and mechanical effects of nickel and manganese on high strength steel weld metals. In S. A. David and T. DebRoy, editors, *Trends in Welding Research*, pages 695–700. ASM, USA, 2002.

[23] E. Keehan, L. Karlsson, H.-O. Andrén, and H. K. D. H. Bhadeshia. Influence of C, Mn and Ni on strong steel weld metals: Part 2, increased impact toughness. *Science and Technology of Welding and Joining*, 11:9–18, 2006.

[24] E. Keehan, L. Karlsson, H.-O. Andrén, and H. K. D. H. Bhadeshia. Influence of C, Mn and Ni on strong steel weld metals: Part 3, increased strength. *Science and Technology of Welding and Joining*, 11:19–24., 2006.

[25] J. S. Byun, J. H. Shim, Y. W. Cho, and D. N. Lee. Non-metallic inclusion and intragranular nucleation of ferrite in Ti-killed C–Mn steel. *Acta Materialia*, 51:1593–1601, 2003.

[26] G. I. Rees and H. K. D. H. Bhadeshia. Thermodynamics of acicular ferrite nucleation. *Materials Science and Technology*, 10:353–358, 1994.

[27] A. R. Mills, G. Thewlis, and J. A. Whiteman. Nature of inclusions in steel weld metals and their influence on the formation of acicular ferrite. *Materials Science and Technology*, 3:1051–1061, 1987.

[28] T. Yamada, H. Terasaki, and Y. Komizo. Relation between inclusion surface and acicular ferrite in low carbon low alloy steel weld. *ISIJ International*, 49:1059–1062, 2009.

[29] E. Keehan, L. Karlsson, H.-O. Andrén, and L-E. Svensson. New developments with C–Mn–Ni high strength steel weld metals: Properties. *Welding Journal, Research Supplement*, 85:211s–218s, 2006.

[30] E. Keehan. Microstructure and properties of novel high strength steel weld metals. *Welding Research Abroad*, 52:1–13, 2006.

[31] E. Keehan, L. Karlsson, M. Thuvander, and E.-L. Bergquist. Microstructural characterisation of as-deposited and reheated weld metal – high strength steel weld metals. *Welding in the World*, 51:44–49, 2007.

[32] H. K. D. H. Bhadeshia. *Bainite in Steels, 2nd edition*. Institute of Materials, London, 2001.

[33] R. W. K. Honeycombe and H. K. D. H. Bhadeshia. *Steels: Microstructure and Properties, 2nd edition*. Butterworths–Hienemann, London, 1995.

[34] G. Nolze. Characterisation of the fcc/bcc orientation relationship by EBSD using pole figures and variants. *Zietschrift für Metallkunde*, 95:744–755, 2004.

[35] 10.J. Börjesson, J. Zachrisson, and L. Karlsson. The role of Ni in high strength low alloy weld metals. In *2nd International Conference on Super High Strength Steels, Italy*, Argentina, 2010. Tenaris.

[36] M. Moll. Stainless steel 2010 and beyond – the bumpy road to recovery, stainless steel world annual procurement report 2010. Technical report, KCI Publishing B. V., Netherlands, 2010.

[37] L. Karlsson, C. Gillenius, H. Arcini, and E. L. Bergquist. Alloying concepts for lean duplex stainless steel weld metals. In *Proc. 6th European Stainless Steel Conference – Science and Market, Helsinki, Finland*, pages 817–822, 2008.

[38] L. Karlsson, H. Arcini, E. L. Bergquist, J. Weidow, and J. Börjesson. Effects of alloying concepts on ferrite morphology and toughness of lean duplex stainless steel weld metals. *Welding in the World*, page in press., 2011.

[39] J. W. Abitbol Meneezes, H. Abreu, S. Kundu, H. K. D. H. Bhadeshia, and P. M. Kelly. .: Crystallography of widmanstẗten austenite in duplex stainless steel weld metal. *Science and Technology of Welding and Joining*, 14:4–10, 2009.

[40] S. Wessman, L. Karlsson, and R. Pettersson an A. Östberg. Study of the influence of tungsten in superduplex stainless steel welds. In *Proceedings of Duplex World 2010*, Beaune, France, 2010.

[41] L. Karlsson. Welding duplex stainless steels - old truths and new grades. In *Proceedings of Duplex World 2010*, Beaune, France, 2010.

[42] T. G. Gooch. Corrosion behaviour of welded stainless steel. *Welding Journal, Research Supplement*, 75:135s–154s, 1996.

[43] B. Sundman, B. Jansson, and J. O. Andersson. The Thermo-Calc databank system. *CALPHAD*, 9:153–190, 1985.

[44] M. Thuvander, L. Karlsson, and B. Munir. Controlling segregation in nickel-base weld metals by balanced alloying. In *Stainless Steel World*, France, 2004. International Institute of Welding.

[45] G. Digiacomo. Residual stresses in high-strength steel weldments and their dimensional stability during welding and stress relieving. *Materials Science and Engineering*, 4:133–145, 1969.

[46] N. Urabe, A. Yoshitake, and H. Kagawa. Effect of welding residual stress on fatigue and fracture toughness. In *Fourth International Offshore Mechanics and Arctic Engineering Symposium*, volume 1, pages 190–195, New York, USA, 1985. American Society of Mechanical Engineers.

[47] H. V. Cordiano. Effect of residual stress on the low cycle fatigue life of large scale weldments in high strength steel. *Journal of Engineering for Industry, A.S.M.E.*, 92:86–92, 1970.

[48] Y.-S. Yang, K.-J. Son, S.-K. Cho, S.-G. Hong, S.-K. Kim, and K.-H. Mo. Effect of residual stress on fatigue strength of resistance spot weldment. *Science and Technology of Welding and Joining*, 6:397–401, 2001.

[49] W. K. C. Jones and P. J. Alberry. A model for stress accumulation in steels during welding. *Metals Technology*, 11:557–566, 1977.

[50] A. Ohta, N. Suzuki, Y. Maeda, K. Hiraoka, and T. Nakamura. Superior fatigue crack growth properties in newly developed weld metal. *International Journal of Fatigue*, 21:S113–S118, 1999.

[51] A. Ohta, O. Watanabe, K. Matsuoka, C. Shiga, S. Nishijima, Y. Maeda, N. Suzuki, and T. Kubo. Fatigue strength improvement by using newly developed low transformation temperature welding material. *Welding in the World*, 43:38–42, 1999.

[52] A. Ohta, N. Suzuki, and Y. Maeda. In A. Meike, editor, *Properties of Complex Inorganic Solids 2*, pages 401–408. Kluwer Academic/Plenum Publishers, 2000.

[53] P. J. Withers and H. K. D. H. Bhadeshia. Residual stress part 1 - measurement techniques. *Materials Science and Technology*, 17:355–365, 2001.

[54] P. J. Withers and H. K. D. H. Bhadeshia. Residual stress part 2 - nature and origins. *Materials Science and Technology*, 17:366–375, 2001.

[55] A. Ohta, K. Matsuoka, N. T. Nguyen, Y. Maeda, and N. Suzuki. Fatigue strength improvement of lap welded joints of thin steel plate using low transformation temperature welding wire. *Welding Journal, Research Supplement*, 82:77s–83s, 2003.

[56] J. Eckerlid, T. Nilsson, and L. Karlsson. Fatigue properties of longitudinal attachments welded using low transformation temperature filler. *Science and Technology of Welding and Joining*, 8:353–359, 2003.

[57] H. Lixing, W. Dongpo, W. Wenxian, and Y. Tainjin. Ultrasonic peening and low transformation temperature electrodes used for improving the fatigue strength of welded joints. *Welding in the World*, 48:34–39, 2004.

[58] S. Zenitani, N. Hayakawa, J. Yamamoto, K. Hiraoka, Y. Morikage, T. Yauda, and K. Amano. Development of new low transformation temperature welding consumable to prevent cold cracking in high strength steel welds. *Science and Technology of Welding and Joining*, 12:516–522, 2007.

[59] J. A. Francis, H. J. Stone, S. Kundu, R. B. Rogge, H. K. D. H. Bhadeshia, P. J. Withers, and L. Karlsson. Transformation temperatures and welding residual stresses in ferritic steels. In *Proceedings of PVP2007, ASME Pressure Vessels and Piping Division Conference*, pages 1–8, San Antonio, Texas, 2007. American Society of Mechanical Engineers, ASME.

[60] Ph. P. Darcis, H. Katsumoto, M. C. Payares-Asprino, S. Liu, and T. A. Siewert. Cruciform fillet welded joint fatigue strength improvements by weld metal phase transformations. *Fatigue and Fracture of Engineering Materials and Structures*, 31:125–136, 2008.

[61] M. C. Payares-Asprino, H. Katsumoto, and S. Liu. Effect of martensite start and finish temperature on residual stress development in structural steel welds. *Welding Journal, Research Supplement*, 87:279s–289s, 2008.

[62] H. Dai, J. A. Francis, H. J. Stone, H. K. D. H. Bhadeshia, and P. J. Withers. Characterising phase transformations and their effects on ferritic weld residual stresses with X–rays and neutrons. *Metallurgical & Materials Transactions A*, 39:3070–3078, 2008.

[63] Y. Mikami, Y. Morikage, M. Mochizuki, and M. Toyoda. Angular distortion of fillet welded T joint using low transformation temperature welding wire. *Science and Technology of Welding and Joining*, 14:97–105, 2009.

[64] H. K. D. H. Bhadeshia. Possible effects of stress on steel weld microstructures. In H. Cerjak and H. K. D. H. Bhadeshia, editors, *Mathematical Modelling of Weld Phenomena – II*, pages 71–118, London, U.K., 1995. Institute of Materials.

[65] A. A. Shirzadi, H. K. D. H. Bhadeshia, L. Karlsson, and P. J. Withers. Stainless steel weld metal designed to mitigate residual stresses. *Science and Technology of Welding and Joining*, 14:559–565, 2009.